

Band lineup and electric fields in $(\alpha\text{-Sn})_m/(\text{CdTe})_n$ [001] and [110] superlattices

A. Continenza* and A. J. Freeman

Department of Physics and Astronomy and Materials Research Center, Northwestern University, Evanston, Illinois 60208-3112

(Received 15 February 1991)

Results of a systematic study of the electronic properties of $(\alpha\text{-Sn})_m/(\text{CdTe})_n$ [001] and [110] superlattices ($m, n = 2, 3$) using the full-potential linearized augmented-plane-wave method are presented. For several different structures we found that $\alpha\text{-Sn}$ is not able to screen the charge piled up at the polar interface and so gives rise to high electric fields. The heat of formation of the unreconstructed [100] interface drops as the period n is increased, but is still considerably higher than other polar unreconstructed and reconstructed interfaces. We find that the band offset is affected by orientation effects only by ~ 0.2 eV and that the lineup for the nonpolar [110] is the average of the two possible unreconstructed [100] interfaces.

I. INTRODUCTION

Semiconductor heterostructures have been the subject of many and extensive theoretical studies,¹⁻⁷ but only very recently has the problem of reconstruction and compensation at *polar* interfaces been the focus of many different experimental and theoretical studies.⁸⁻¹⁰ In particular, papers have appeared recently on the Ge/GaAs [111] and [001] (Refs. 3, 11, and 12) polar interfaces aimed at investigating the properties and the potential technological implications that structures with possible built-in electric fields may have; the effects due to strain-induced electric fields on the optical properties of superlattices also have been extensively studied.¹³ In addition, considerable attention has been devoted^{4,5,14-18} to heterostructures of $\alpha\text{-Sn}/\text{CdTe}$ with the intent of obtaining a narrow-band-gap material and, at the same time, heterostructures with larger band offsets than HgTe/CdTe. Several studies in fact have addressed the issue of the band-gap opening of $\alpha\text{-Sn}$ by quantum size effect¹⁷⁻¹⁹ and some experimental¹⁸ works were able to confirm that there is, indeed, the possibility to obtain a material with a band gap that can be even smaller than that in InSb. Such a property is, in fact, desirable for device applications—particularly for infrared detectors.

In a previous study,²⁰ we focused on the structural and electronic properties of order ultrathin superlattices of $\alpha\text{-Sn}/\text{CdTe}$. We found that the monolayer superlattices have a direct nonzero band gap and that the heat of formation (even for the “compensated” structure) is still quite high [~ 0.97 eV/(4 atoms)]. In the present study we investigate the electronic properties and the potential lineup at the interface between $\alpha\text{-Sn}$ and CdTe. In particular, we are interested in exploring how the valence-band offset is affected by the orientation (and therefore by the polarity) of the interface and whether $\alpha\text{-Sn}$ gives rise to high internal electric fields (as is the case for Ge in the analogous Ge/GaAs interface) or rather, being a semimetal, if it is able to screen the excess charges at the interface bonds by mean of a Schottky-barrier-like behavior. To answer this question, we present results of a sys-

tematic study of $(\alpha\text{-Sn})_m/(\text{CdTe})_n$ superlattices (for $n, m = 1, 2, 3$) for two different orientations: the polar [001] and the nonpolar [110] interface. In order to understand better how the charges redistribute at the interface, we study three different cases for the [001] orientation: the Cd-terminating interface, the Te-terminating interface (for which we also calculated the 2×2 superlattice), and the superstructure in which both interfaces are allowed [$(\text{Sn}_4)/(\text{CdTe})_2$]. The fundamental difference between them is that, while in the first two cases no electric field can exist, in the latter case, a built-in electric field is allowed by symmetry.

This paper is organized as follows: we discuss details of our calculation in Sec. II, present results for the stability of the superlattices considered in Sec. III, discuss the charge redistribution and the internal electric fields in Sec. IV, the band lineup in Sec. V, and, finally, present our conclusions in Sec. VI.

II. METHODOLOGY AND APPROACH

A. Structural details

$\alpha\text{-Sn}/\text{CdTe}$ is a very-well-matched heterostructure (the experimental mismatch between the two lattice constants is only 0.14%). In a previous study,²⁰ which focused on the electronic and structural properties of pure $\alpha\text{-Sn}$, CdTe, and some of their ultrathin superlattices, we found that our calculation does not reproduce too well the experimental lattice mismatch (we found $\sim 1.0\%$ mismatch) due to an overestimate of the ground-state bond length in pure $\alpha\text{-Sn}$. From a total-energy study, we also found that substitution of Cd by Sn in the CdTe lattice causes large tetragonal distortions (the equilibrium Sn-Te bond length is found to be 10% larger than the covalent Sn-Sn and Cd-Te bond lengths), while substitution of Te by Sn gives rise to a more covalent bond that follows bond-length conservation within 2%.

The present paper is focused on the study of the $(\alpha\text{-Sn})_m/(\text{CdTe})_n$ interface and on how the potential lineup and the band offset are affected by the interface orientation.

To this end, we considered an ideal and well-matched interface, in which local bond-length distortions due to the interface are neglected. Of course, we are aware of the limitations that this assumption may impose on the band-lineup results, since bond-length relaxation and interface compensation can strongly affect the interface-dipole potential as well as the enthalpy of formation of each structure. On the other hand, we should recall that experiments^{15–17} seem to find an abrupt interface even for the polar [001] interface and that they were able to rule out any diffusion of Cd into the Sn layers and the formation of intermixed compounds (as, for example, SnTe). Nevertheless, a complete total-energy study of all the unknown parameters should be undertaken as a second step, once other more crucial questions (regarding, for example, the interface-orientation effects on the valence-band offset) have been studied.

We therefore considered well-matched structures built up by ideal zinc-blende unit cells with lattice constant equal to the average of the calculated ground-state lattice constants for α -Sn and CeTe [$a_0 = 6.505 \text{ \AA}$ (Ref. 20)]. The [001] superlattices have tetragonal structure with a unit cell that is a square in the x - y plane and has edges equal to $a = a_0/\sqrt{2}$. The 3×3 [110] superlattice has an orthorhombic cell that in the plane perpendicular to the growth direction is a rectangle with edges, $a = a_0/\sqrt{2}$ and $b = a_0$; the period c along the growth direction is given by $c = 3a_0/\sqrt{2}$.

B. Computational details

We perform all-electron calculations using the full-potential linearized augmented-plane-wave method²¹ and make use of the local-density approximation to the density-functional theory as parametrized by Hedin and Lundqvist.²² The core states are calculated fully relativistically and updated at each iteration, whereas for the valence states a scalar-relativistic calculation is performed; the spin-orbit effect on the valence-band offset is calculated as a correction estimated from results obtained from the pure constituents.²⁰

We considered equal-sphere radius values for Cd, Sn, and Te ($R_{\text{MT}} = 2.5 \text{ a.u.}$), and used a wave-function cutoff, $k_{\text{max}} = 2.8 \text{ a.u.}$ for all the superlattices considered (this wave-function cutoff gives 529 and 1045 basis functions at the center of the Brillouin zone for the 2×2 and 3×3 [001], respectively). The wave function and the potential inside the muffin-tin spheres were expanded in spherical harmonics up to $l_{\text{max}} = 6$. In the present calculations, the Sn $4d$ and Te $4d$ states are considered as part of the core whereas the Cd $4d$ states are considered as valence. However, since about 0.16 and 0.05 electrons spill out of each Sn and Te sphere, respectively, and since the shape of the potential across the interface is very sensitive to the way this charge is redistributed, we describe the core charge spilling out of the muffin-tin spheres by mean of an exact overlapping-charge method.²³ We performed several tests on the convergence with respect to the wave-function cutoff and found that the valence-band offset evaluated by choosing the Cd core levels as reference energies, was highly sensitive to the k_{max} value used,

if its value was below $k_{\text{max}} = 2.7 \text{ a.u.}$ This is due to the presence of the shallow Cd $4d$ states and to the fact that the wave-function basis set needed to correctly describe these states has to be quite large. The same sensitivity was not found in the case of the Te and Sn core levels (the energy difference between two different core levels was very stable, within 0.006 eV, even for k_{max} as low as 2.5 a.u.). From our tests, we were able to estimate that the error in the valence-band offset caused by a limited wave-function set was about 0.05 eV if the Cd core states were chosen as reference energy levels.

We also performed tests regarding the treatment of the Cd $4d$ states. In particular, we found that the treatment of these states as part of the core would have implied a far too large amount of charge spilling out of the muffin-tin spheres (about 0.6 electron per each Cd atom), making the convergence slower and harder.

The [001] superlattices (for $n = 2, 3$) have simple tetragonal symmetry and D_{2d}^5 space group; the 3×3 [110] superlattice, as well as the [001] superlattice containing both interfaces, has a simple orthorhombic cell and C_{2v}^1 space group. Integrations over the irreducible wedge of the Brillouin zone (BZ) were performed using 3 and 6 special \mathbf{k} points^{24–26} for the simple tetragonal cells and 4, 8, and 16 \mathbf{k} points for the orthorhombic cell; the results shown are those obtained using 3 \mathbf{k} points (4 \mathbf{k} points for the orthorhombic cells), since the effect of a different BZ sampling on the core-level binding-energy differences was smaller than 0.01 eV.

In order to assure consistency in comparing the reference-energy levels between the superlattices and the pure constituents, we calculated the reference equilibrium structures of Sn and CdTe using the same geometrical structure, the same numerical parameters, and the same treatment of the Cd $4d$ states used for the superlattices.

III. STABILITY

Table I shows the enthalpy of formation for some of the structures considered, calculated by comparing the total energy of the supercells with those of the pure constituents, in the same geometries and with the same convergence parameters. We found that the enthalpy of formation per unit cell decreases quite remarkably as the periodicity n is increased; as expected, the nonpolar interface is more stable and the enthalpy of formation drops dramatically as the periodicity is increased. Still we should expect the unreconstructed 3×3 [100] superlattice to be less stable than the 3×3 [110] superlattice, on the basis of other theoretical calculations²⁷ performed on similar polar interfaces. In the [110] interfaces, charges with opposite sign (due to the nonoctet bonds) are confined within the same plane and this lowers the electrostatic energy with respect to the [001] configuration in which the unbalanced holes or electrons lie in different and separated interface planes.

However, it is also reasonable to expect that bond relaxation and reconstruction at the interface (for example, the exchange per cell of a Sn atom with a Cd or a Te)—not considered in our calculation—will reduce the heat of formation even further, affecting more sensibly the po-

TABLE I. Enthalpy of formation ΔH [in units of eV/(4 atoms)] calculated for some of the structures considered. Our accuracy is ± 0.015 eV.

	ΔH
Sn_2/CdTe [110]	0.938
$\text{Sn}_6/(\text{CdTe})_3$ [110]	0.295
Sn_2/CdTe [100]	0.938
$\text{Sn}_4/(\text{CdTe})_2$ [100]	0.543

lar interface. The calculated formation enthalpies are quite high when compared with other heteropolar superlattices, for which some calculations are available [see, for example, some $A^{\text{IV}}/B^{\text{III}}C^{\text{V}}$ systems such as unreconstructed Si/GaP,²⁷ Si/GaAs,²⁷ and Ge/GaAs (Refs. 3 and 27); this can be explained by considering that the “uncompensated” charge per bond in the $A^{\text{IV}}/B^{\text{III}}C^{\text{VI}}$ superlattices is twice as large as that of the $A^{\text{IV}}/B^{\text{III}}C^{\text{V}}$ junction. Still the differences in formation enthalpy are not that large (the 3×3 [110] superlattice has an enthalpy of formation only ~ 0.2 eV higher than Ge/GaAs according to the value reported in Ref. 27 and even comparable to the calculation in Ref. 3), so it is expected that these structures can be stabilized and processed for device application—as suggested by Reno and Stephenson.²⁸

IV. CHARGE DISTRIBUTIONS AND ELECTRIC FIELDS

Before discussing the valence-band offset, let us discuss some results concerning the charge redistribution at the interface and the potential profile across the junction for the structures considered, namely, superlattices with periodicity n up to $n=3$, for which we found that the bulk behavior was recovered in the inner layers. This is well described by our macroscopic average of the planar average-charge density, defined according to Ref. 6 using the equations

$$\bar{\rho}(z) = \frac{1}{A} \int_A \rho(x, y, z) dx dy \quad (1)$$

and

$$\langle \rho(z) \rangle = \int_{z-c_b/2}^{z+c_b/2} \bar{\rho}(z') dz' . \quad (2)$$

The periodicity c_b of the macroscopic averaging process is equal to half the value of the zinc-blende lattice constant for the [001] and to $a_0/\sqrt{2}$ for the [110] superlattice, respectively. The macroscopic averages of the charge density are shown in Figs. 1, 2, and 3 for the [001] Te-rich, [001] Cd-rich, and the [110] structures, respectively; in all cases, the charge tends to the perfectly flat bulk value in the layers away from the interface (see Figs. 1–3, solid lines). (Note that the quantities plotted in these figures are centered around zero since they represent the valence charge from which the corresponding nuclear contribution was subtracted out, therefore resulting in a net neutral charge.) From the macroscopic average of the charge density it is possible to derive a one-dimensional Poisson equation to obtain the macro-

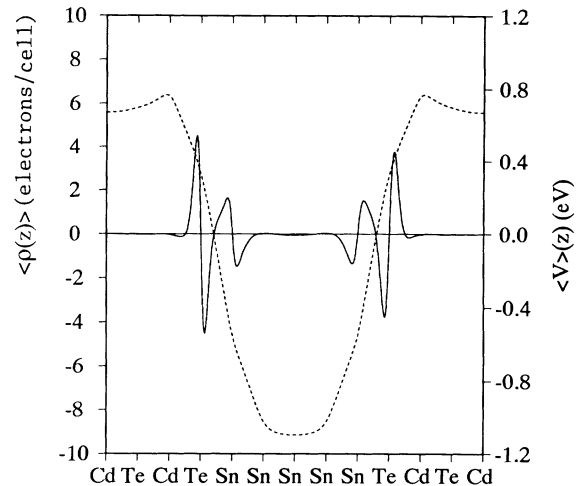


FIG. 1. Macroscopic averages of the valence charge density (solid line) and electrostatic potential (dashed line) in the Te-rich structure.

scopic electrostatic potential as a function of the z coordinate⁶ (chosen to be parallel to the growth direction). The macroscopic average of the potential is shown in Figs. 1–3 (dashed lines) for some of the structures studied. As expected the average potential is flat and constant in the “bulk” regions for the [110] and both the Cd- and Te-rich [001] structures. The disturbances caused by the interface are well confined, in the [110] case, within the interface layer (the charge density and the potential recover completely their bulk value in the layer underneath the interface), while they are more widely spread in the [001] structures. In this latter case, the “bulk” regions are quite small and the interface dipole extends for a few monolayers across the interface; moreover, the potential is flat in the inner bulk regions, giving rise to a zero electric field—as required by symmetry.

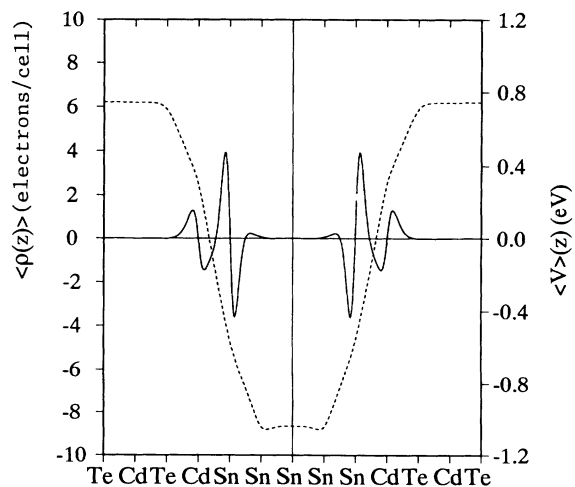


FIG. 2. Macroscopic averages of the valence charge density (solid line) and electrostatic potential (dashed line) in the [001] Cd-rich structure.

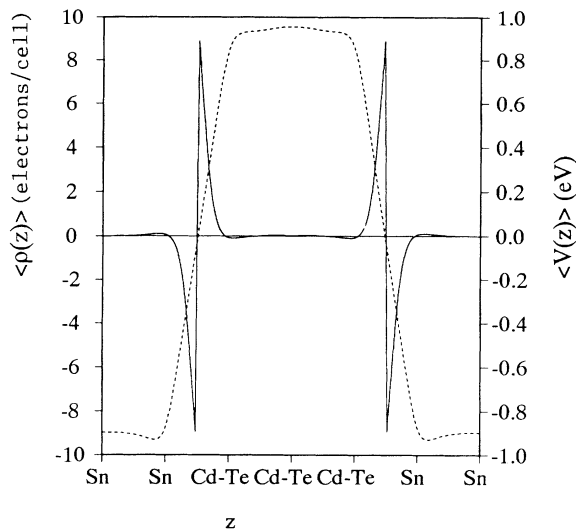


FIG. 3. Macroscopic averages of the valence charge density (solid line) and electrostatic potential (dashed line) in the [110] structure.

However, if we consider the structure in which symmetry allows a net electric field (i.e., for example, the [001] $\text{Sn}_4/\text{CdTe}_2$ structure), we find that the uncompensated charge of the “nonoctet” interface bonds, piles up at the interfaces and gives rise to quite a large electric field \bar{E} which is not completely screened, not even in the semimetal region ($\bar{E}_{\text{Sn}} \sim 0.19 \text{ V/\AA}$). This shows that the [001] interface should not be an abrupt interface, and that compensation may occur at the interface so as to lower this charge accumulation and consequently make the electric field vanish into the bulk regions. By using a crude estimate (i.e., by integrating the planar-averaged charge density in either sides of the junction), we find that $0.90 + 0.02$ valence electrons are accumulated in the Sn-Te interface layer, while the same amount of charge is lacking in the Cd-Sn layer; this value is remarkably close to the unbalanced charge in the “nonoctet” interface bonds (i.e., one electron per cell). This excess charge on both interfaces (Sn-Cd and Sn-Te) is shown quite clearly in Fig. 4, where the macroscopic average of the total charge (including the neutralizing nuclear contributions) is plotted.

When we include the neutralizing nuclear contributions, we find that some positive charge is accumulated into the Sn-Te bond, while some negative charge is piled up along the Sn-Cd bond. One can easily understand this, using a virtual crystal-like picture (following Ref. 10) and considering an ideal crystal made up with two alternating ionic types (bearing charge $+3e$ and $+5e$, respectively). If now a perturbation is applied such that one electron charge is alternately subtracted and added, the crystal will become a sequence of $2+$ and $6+$ ions (in the CdTe side); at the interface, though, in order to recover the $4+$ Sn ions (in the other side of the junction), the perturbation has to change phase (i.e., it will add $1+$ to the ion with $3+$ charge and subtract $1-$ from the ion with $5+$ charge). This will result in consecutive $1+$

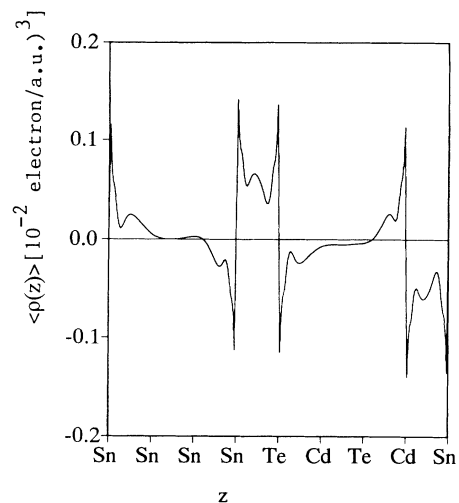


FIG. 4. Macroscopic average of the valence charge density and the corresponding nuclei neutralizing contribution for the [001] superstructure containing both Cd and Te-terminating interfaces.

charges on the Sn-Te and $1-$ on the Cd-Sn interfaces, respectively. As is clear from the plot (see Fig. 4), this ionic charge is not completely screened by the electronic bonding charge and it results in a net positive (negative) charge on the macroscopic average charge-density plot, along the Sn-Te (Cd-Sn) interface bond. It is the uncompensated amount of charge that is responsible for the electric field. By integrating Poisson’s equation, we can calculate the electric field and the potential generated by this charge. The electric field (see Fig. 5) goes from the positive (Sn-Te) toward the negative (Sn-Cd) side according to the usual convention and reaches a constant value, $\bar{E}_{\text{Sn}} \approx 0.19 \pm 0.02 \text{ V/\AA}$ in the Sn bulk region. An analogous evaluation of the electric field in the CdTe region is not possible due to the fact that, in the structure con-

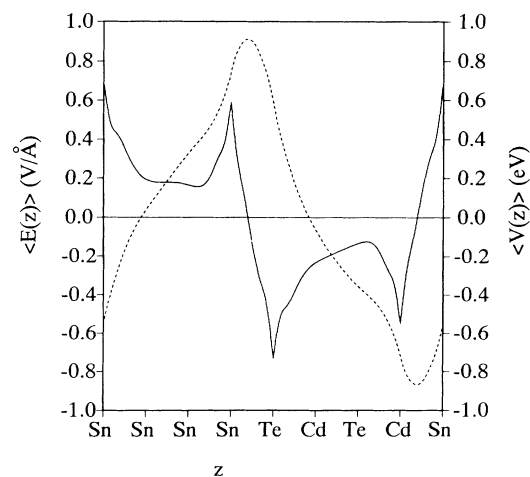


FIG. 5. Macroscopic averages of the electric field (solid line) and electrostatic potential (dashed line) in the [001] structure containing both Cd and Te-terminating interfaces.

sidered, the CdTe layer is not thick enough to stabilize the electric field; we can roughly estimate a value \bar{E}_{CdTe} between $\sim 0.1-0.2 \text{ V}/\text{\AA}$. We will not discuss here how this huge electric field may affect the optical properties of the system, since this is not the aim of the present work; we remark that this subject has been recently studied, in the case of a strain-induced field, by Smith and Mailhot.¹³

V. BAND LINEUP

A. Results

For some of the superlattices considered, we calculated the valence-band offset by using the core levels as reference energy levels and also the macroscopic-averages method.⁶ The definition of a band offset in the case of the [001] structures may not seem appropriate since, as discussed above, the abrupt [001] interface should not be stable and, in addition, for the superlattice containing both interfaces it is impossible to define a valence-band offset due to the electric field present in the bulk regions. However, in order to study the orientation and interface dependence, we considered the potential alignment in the two sides of the interface for the [001] structures in which no electric field is allowed by symmetry. The study of a “compensated” structure, with a mixed Sn-Te or Sn-Cd interface layer would have implied a doubling of the unit cell and a consequently larger computational effort. It is our opinion that a comparison of the valence-band offset in these different structures can give us valuable hints on the role played by the chemistry and interface compensation on the potential lineup.

Due to the less accurate convergence of the Cd levels discussed above, we considered as reference levels the core levels of Te and Sn (for completeness, however, we report in Table II also the values relative to the Cd states; the resulting valence-band offset is indicated as $\Delta E_v^{\text{Sn-Te}}$ and $\Delta E_v^{\text{Sn-Cd}}$, respectively).

We remark that all the structures considered have me-

tallic character, due to the severe underestimate of the band gap within local-density approximation (LDA), and therefore one should probably talk about Schottky barriers, rather than valence-band offsets. However, from our calculations and considering a rough estimate of the LDA error (starting from the band-gap correction found in the pure constituents), we believe that there is a band-gap opening and that the gap is direct (at least for the [001] structures). This would agree with some recent experimental findings¹⁸ that confirmed the band-gap opening via resistivity measurements and with some earlier experiments¹⁵ that found evidence of the existence of empty quantum-well states from the shape of the inelastic-scattered electron tail (in low-energy electron-loss experiments). Nevertheless, the errors made in these kinds of evaluations are such that speaking about reliable values for the band gap is still not appropriate; we will therefore refer to “band lineup” in a more general and broader meaning. Moreover, the nonperfect metallic behavior of α -Sn is well shown by the presence of a constant electric field in the Sn region in the [001] $\text{Sn}_4/(\text{CdTe})_2$ structure.²⁹

The calculated band-lineup values, obtained using the core levels as reference energy levels in analogy with the procedure used by x-ray photoemission spectroscopy experiments and our earlier studies^{1,30} and including the spin-orbit correction ($\Delta E_v^{\text{r.o.}}$), are summarized in Table III; the spin-orbit correction has been added by considering the spin-orbit correction in the pure constituents²⁰ and taking into account that the relative shift of the two valence-band maxima is given by $\frac{1}{3} \times \frac{1}{2} (\Delta_{\text{s.o.}}^{\text{CdTe}} - \Delta_{\text{s.o.}}^{\text{Sn}})$. The errors associated with the values shown in Table III take into account the uncertainty related to the Cd $4d$ levels and, in the case of the [110] interface, the difference in the offset related to considering different atomic “bulk” sites. As is well known, the core levels are very sensitive to the chemical environment and in fact the core levels of Sn_1 , (i.e., the “bulk” site belonging to the Te-Sn-Sn-Sn-Te bonding chain) are constantly 0.008 mRy lower than those of Sn_2 (i.e., the site belonging to the Cd-Sn-

TABLE II. Core energy differences and corresponding valence-band offsets ΔE_v (in eV) for the $n=2,3$ superlattices considered.

Core state	2×2		3×3	
	$\Delta E_v^{\text{Sn-Te}}$	$\Delta E_v^{\text{Sn-Cd}}$	$\Delta E_v^{\text{Sn-Te}}$	$\Delta E_v^{\text{Sn-Cd}}$
Te-rich	1s	1.04	1.02	1.08
	2s	1.04	1.03	1.07
	3s	1.04	1.03	1.04
	4s	1.04	1.02	1.01
Cd-rich	1s		0.90	0.93
	2s		0.90	0.92
	3s		0.90	0.90
	4s		0.90	0.90
[110]	1s		0.97	1.16
	2s		0.98	1.14
	3s		0.97	1.13
	4s		0.97	1.12

TABLE III. Core energy differences and corresponding valence-band offsets ΔE_v (in eV) for the $n=2,3$ superlattices considered. $\Delta E_v^{s.o.}$ denotes the spin-orbit corrected ΔE_v values.

	2×2		3×3		Δ
	ΔE_v	$\Delta E_v^{s.o.}$	ΔE_v	$\Delta E_v^{s.o.}$	
Te-rich	1.04	1.10	1.03	1.09	± 0.02
Cd-rich			0.90	0.96	± 0.02
[110]			0.97	1.03	± 0.1

Sn-Sn-Cd bonding chain).

Before discussing the comparison with experiment, let us also discuss the results obtained using the macroscopic-average technique. The macroscopic average of the potential is shown in Figs. 1, 2, and 3 (dashed lines) for the Te-rich [001], Cd-rich [001], and 3×3 [110] structures, respectively. It is clear from the potential profile, that the interface region (defined as the region in which the bulk properties are not recovered) extends over three layers which is a quite large spatial region ($\sim 5 \text{ \AA}$), in the uncompensated [001] interface, much larger than that observed in the nonpolar [110] interface or in other heterojunctions (see, for example, the InAs/InP case³⁰ where the interface region extended only for one layer, 1.5–2 \AA). This is due to the fact that the atomic layer at the interface (i.e., the Te-Sn or the Cd-Sn layer) contains nonoctet bonds and it is therefore not bulklike, not even from the atomic composition point of view, its nonbulk behavior causes strong disturbances in the calculated macroscopic quantities and introduces rapidly varying oscillations that can be easily seen in Figs. 1 and 2.

Of course, this is a consequence of the particular geometry assumed and may not well represent the actual situation, in which the abruptness and the discontinuity introduced by the assumption of such a sharp interface can be smoothed out by interface reconstruction or compensation. We recall, in fact, that in a similar but compensated interface (GaAs/Ge), the interface region was still very well confined to one layer.³¹

However, our crude model for this interface can still show features that can shed light on the real material. We note, for example, that the width of the interface region is independent of the chemistry of the interface, and the potential profile is almost the same for both Te- and Cd-terminating interfaces. However, what is changed in going from one structure to the other is the potential profile inside the CdTe region: in the case of the Cd-rich

structure (see Fig. 2) the potential is perfectly flat in both the bulk regions, whereas in the Te-rich structure (see Fig. 1) it shows a well defined nonconstant shape in the CdTe region. This implies that there is a finite nonzero electric field over the entire CdTe region which is not completely screened, even though the total field has to be zero by symmetry. It therefore seems that the Cd-Sn bonding, being more covalent, is able to provide a better screening (in the CdTe region) to the unbalanced charge piled up at the interface. The more ionic Te-Sn bond, on the other hand, provides a larger charge transfer and a larger dipole localized in the CdTe layer which is not well screened in the layers away from the interface. The valence-band-offset values evaluated by using the macroscopic averages are shown in Table IV. Here, ΔV_v and ΔV_{core} represent the macroscopic average of the potential jump across the interface due to the valence and core electrons, respectively; ΔE_{bin} denotes the difference of the average potential, referred to the valence-band maximum (VBM) in the binary constituents, and, finally, $\Delta E_v^{s.o.}$ refers to the spin-orbit-corrected ΔE_v values. The computational error (Δ), given in the table, takes into account the numerical uncertainty associated with the averaged process and the representation of the nuclear charge as finite-width Gaussians, in order to simulate the nuclear “pointlike” charges.

Let us point out a few important aspects. As a first remark, we note that there is a noticeable difference between the two [001] structures which is related to both contributions, the potential lineup due to the core part and to the valence charge. The dependence of the core distribution from the interface is, of course, a consequence of the large electrostatic term due to the different charge concentration in the two materials in the two cases (Te or Cd excess); the variations in the valence contribution are a result of the different chemical and bonding properties of the interfaces. We also notice that the lineup for the [110] orientation is actually the average of the [100] Te- and Cd-terminating interfaces. The valence-band-offset values calculated using the macroscopic averages are in good agreement (within 0.1 eV) with the results obtained using the core levels as reference energies (see Tables III and IV).

B. Comparison with experiment

Let us now turn to a comparison of the theoretical results (summarized in Table III) with the experimental

TABLE IV. Quantities (in eV) used in the evaluation of the valence-band offsets ΔE_v . Here ΔV_v and ΔV_{core} are differences of the macroscopic average of the potential on the two sides of the interface due to the valence and core electrons, respectively; ΔE_{bin} denotes the difference of the average potential, referred to the VBM, in the binary constituents, $\Delta E_v^{s.o.}$ are the spin-orbit corrected ΔE_v values and Δ represents the accuracy of our results.

	ΔE_{bin}	ΔV_{core}	ΔV_v	ΔE_v	$\Delta E_v^{s.o.}$	Δ
Te-rich	1.45	−2.10	1.82	1.17	1.23	0.05
Cd-rich	1.45	−2.21	1.75	0.99	1.05	0.05
[110]	1.45	−2.23	1.85	1.07	1.13	0.05

data available on the valence-band offset of these heterojunctions.

The valence-band offset has been measured for various different growth directions ([001],¹⁶ [110],¹⁵ and [111] (Ref. 17)); the experimental results are 0.55 ± 0.10 , 1.1 ± 0.1 , and 1.1 ± 0.1 , respectively. It is clear, from the large difference between the experimental values for the [001] and [110] (or [111]) interfaces, that there is a strong dependence on the interface orientation; this dependence is usually attributed to the electric dipole present in the [001] interface which is lacking in the nonpolar [110] interface. It is rather surprising, nevertheless, that the experimental results for the still-polar [111] interface give a band offset which is very close to that of the nonpolar interface [110]. If the interface dipole is responsible for the orientation dependence of the offset for the polar heterojunction, it would be reasonable to expect a comparable deviation of the valence-band offset for the [110] from both the [100] and [111] interfaces. Of course, it should also be taken into account that the interface dipole at the [111] interface could be lower than that at the [100] interface due to the fact that there is only one nonoctet bond per cell. We have to notice, however, that a smaller difference between these same growth directions was observed in the case of Ge/GaAs;¹⁰ in this case, the difference is less than ~ 0.10 eV, considering different kinds of reconstructed interfaces. Moreover, extensive experiments³² performed on similar systems (such as CdS/Ge, ZnSe/Ge, and GaAs/Ge) seem to suggest that the valence-band offset in such a wide variety of systems is independent on growth and orientation conditions within ~ 0.2 eV. We are therefore very cautious in attempting any comparison with experiments as far as the [100] orientation is concerned.

Our calculated values for the [001] interface are much closer to the experimental results for the [111] and nonpolar [110] interface (~ 1.0 eV) than for the polar [001]; moreover, they are also in reasonable agreement with our result and other theoretical calculations for the [110] interface which give $\Delta E_v = 1.0$ – 1.10 eV,⁴ thereby suggesting that there should not be such a large dependence on interface orientation.

C. Discussion

It is hard at this point to draw some definite conclusions: from our calculations, and considering also the previously mentioned theoretical results, it seems that the effect of orientation on the charge readjustment should not be greater than ~ 0.1 eV; this would also be in agreement with calculations on the interface dipole performed by Lambrecht and Segall.⁵ Moreover, considering the offset difference between the Cd interface with respect to the Te-terminating interface, one could also argue that the interface chemistry cannot affect the final lineup by more than ~ 0.2 eV, and that probably the offset of the real interface should be somewhat close to the average of the two different cases considered, if compensation does occur. In this line of reasoning the Te- and Cd-rich structures considered in this work would represent the

two extreme limits that should include the real [100] interface.

Of course there are many other factors that have to be taken into account that have not been fully considered in our present calculation, that can dramatically change the interface-dipole potential and the resulting band lineup, such as interface reconstruction, intermixing, and relaxation. It is reasonable, for example, to expect a quite different value for the offset, if full relaxation of the interface-layer bond lengths is allowed. This would considerably affect the interface dipole and, consequently, the band offset overall if we consider that a full relaxation of the Sn-Te bond may imply large tetragonal distortions.²⁰

Moreover, it is also possible that diffusion at the interface would tend to compensate the interface bonds resulting in a mixed (Sn-Te or Sn-Cd) interface layer. However, the issue related to interface compensation deserves some more discussion. A few years ago, Martin⁸ used a thermodynamic argument to show that the abrupt Ge/GaAs interface is not stable against compensation; he evaluated the energy that stabilizes the formation of compensated interfaces from a knowledge of the enthalpy to create a neutral substitution (ΔH_0) and the energy to place the extra electron (or hole) at an energy E_s with respect to the Fermi level (E_F). In the case of Ge/GaAs he was able to show that the quantity ΔH is always negative since the energy required to “compensate” the interface (ΔH_0) is always less than the energy to accommodate the extra charge at the Fermi level. The validity of this argument has been recently questioned by Bylander and Kleinman,³ who were able to show that the enthalpy of formation of the polar [111] is even smaller than that of the [110] interface, and that the interface-charge imbalance might not be the only cause that drives the system to interface compensation.

In the present case, this argument is even more critical since α -Sn is a zero band-gap semiconductor (even if its gap can be opened by quantum-confinement effects using thin α -Sn layers) and, moreover, the energy necessary to “compensate” the interface (ΔH_0) is expected to be very high, since α -Sn and CdTe do not form stable compounds (it is very hard, in practice to make Sn substitutions in CdTe, while Ge in GaAs can play the role of a good donor and/or acceptor). Therefore one would expect that in the growth process (such as in the case of molecular beam epitaxy or metal-organic chemical-vapor deposition) compound intermixing (or compensation) and diffusion can be inhibited, as some experimental findings seem to suggest.^{15,16,18,28}

VI. CONCLUSIONS

We presented results of a detailed study of the structural and electronic properties of the well-matched polar α -Sn/CdTe [001] and [110] interfaces. We found that in the polar interface large macroscopic electric fields are present that might drive the system toward compensation or interface reconstruction. However, the calculated formation enthalpies for the unreconstructed surfaces are still comparable to those of similar hetero-

lar systems that have been successfully stabilized.

We find evidences for a direct-band-gap opening for α -Sn thin layers grown in the [100] orientation; unfortunately the LDA errors in determining the semiconductor band gap are such that we cannot predict a reliable value.

The band lineup calculated for the two possible unreconstructed (Cd and Te terminating) [100] interfaces (excluding many-body effects) are in agreement with experiments performed for the [111] and [110] interfaces, but they differ significantly from the experimental value for the [100] interface. The difference between the two ideal [100] interfaces is ≈ 0.1 eV showing that there is a dependence on the interface morphology. Nevertheless, these potential lineups are comparable with that for the "compensated" [110] interface suggesting that interface reconstruction is expected not to affect dramatically the overall lineup. We cannot tell, at this point, whether the discrepancy between our calculated result and experiment for the [100] interface is entirely due to the ideal model interface assumed by the calculation or if it is rath-

er a problem with experimental accuracy. We also remark that our results do not include nonlocal effects³³ and that in this particular case, corrections due to the different dielectric and screening properties of the two materials could be significant. However, the good agreement with the experimental results obtained for the [110] interface seem to indicate that such corrections should not dramatically affect our theoretical predictions.

ACKNOWLEDGMENTS

We are very pleased to acknowledge helpful discussions with S. Baroni and R. Resta. We thank J. B. Ketterson and G. K. Wong for suggesting this work and for discussions. The work was supported by the National Science Foundation (through the Northwestern University Materials Research Center, Grant No. DMR88-21571, and by a grant of computer time from its Division of Advanced Scientific Computing at the National Center for Supercomputing Applications, University of Illinois, Urbana/Champaign).

*Present address: Università degli Studi dell'Aquila, Coppito, I-67010, Italy.

¹S. Massidda, B. I. Min, and A. J. Freeman, Phys. Rev. B **35**, 9871 (1987).

²S. H. Wei and A. Zunger, Phys. Rev. Lett. **59**, 144 (1987).

³D. M. Bylander and L. Kleinman, Phys. Rev. B **41**, 3509 (1990).

⁴M. Cardona and N. E. Christensen, Phys. Rev. B **35**, 6182 (1987).

⁵W. R. L. Lambrecht and B. Segall, Phys. Rev. B **41**, 2832 (1990).

⁶A. Baldereschi, S. Baroni, and R. Resta, Phys. Rev. Lett. **61**, 734 (1988).

⁷C. Van de Walle and R. Martin, Phys. Rev. B **35**, 8154 (1987); C. Van de Walle, *ibid.* **39**, 1871 (1989), and references therein.

⁸R. Martin, J. Vac. Sci. Technol. **17**, 978 (1980).

⁹A. K. Kunc and R. Martin, Phys. Rev. B **24**, 3445 (1981).

¹⁰W. A. Harrison, E. A. Kraut, J. R. Waldrop, and R. W. Grant, Phys. Rev. B **18**, 4402 (1978).

¹¹A. Munoz, N. Chetty, and R. M. Martin, Phys. Rev. B **41**, 2976 (1990).

¹²S. Lee, D. M. Bylander, and L. Kleinman, Phys. Rev. B **41**, 10 264 (1990).

¹³D. L. Smith and C. Mailhot, Phys. Rev. Lett. **58**, 1264 (1987); C. Mailhot and D. L. Smith, Phys. Rev. B **35**, 1242 (1987), and references therein.

¹⁴L. W. Tu, G. K. Wong, and J. B. Ketterson, Appl. Phys. Lett. **54**, 1010 (1989).

¹⁵H. Höchst, D. W. Niles, and I. Hernández-Calderón, J. Vac. Sci. Technol. B **6**, 1219 (1988).

¹⁶M. Tang, D. W. Niles, I. Hernández-Calderón, and H. Höchst, Phys. Rev. B **36**, 3336 (1987).

¹⁷S. Takatani and Y. W. Chung Phys. Rev. B **31**, 2290 (1985).

¹⁸L. W. Tu, G. K. Wong, and J. B. Ketterson, Appl. Phys. Lett. **55**, 1327 (1989).

¹⁹B. I. Craig and B. J. Garrison, Phys. Rev. B **33**, 8130 (1986).

²⁰A. Continenza and A. J. Freeman, Phys. Rev. B **43**, 8951 (1991).

²¹H. J. F. Jansen and A. J. Freeman, Phys. Rev. B **30**, 561 (1984).

²²L. Hedin and B. I. Lundqvist, J. Phys. C **4**, 2064 (1971).

²³D. D. Koelling, Solid State Commun. **53**, 1019 (1985).

²⁴A. Baldereschi, Phys. Rev. B **7**, 5212 (1973).

²⁵D. J. Chadi and M. L. Cohen, Phys. Rev. B **8**, 5747 (1973).

²⁶J. Monkhorst and J. D. Pack, Phys. Rev. B **13**, 5188 (1976).

²⁷R. G. Dandrea, S. Froyen, and A. Zunger, Phys. Rev. B **42**, 3219 (1991).

²⁸J. L. Reno and L. L. Stephenson, Appl. Phys. Lett. **54**, 2207 (1989).

²⁹The screening length, obtained within a Thomas-Fermi picture considering the density of state at the Fermi level as previously obtained (Ref. 20) ($\lambda = \sqrt{\pi/[e^2 N(E_F)]} \sim 25 \text{ \AA}$), is equal to about four times the lattice constant (a_0) in α -Sn.

³⁰A. Continenza, S. Massidda, and A. J. Freeman, Phys. Rev. B **42**, 3469 (1990).

³¹S. Baroni, R. Resta, A. Baldereschi, and M. Peressi, in *Spectroscopy of Semiconductor Microstructures*, NATO Advanced Workshop, edited by G. Fasol, A. Fasolino, and P. Lugli (Plenum, New York, 1989).

³²A. D. Katnani, in *Heterojunction Band Discontinuities: Physics and Device Application*, edited by F. Capasso and G. Margaritondo (North-Holland, Amsterdam, 1989).

³³S. B. Zhang, M. L. Cohen, S. G. Louis, D. Tomanek, and M. S. Hybertsen, Phys. Rev. B **41**, 10 058 (1990).